



## Research article

# A conformable mathematical model of Ebola Virus Disease and its stability analysis

Nadeem Abbas<sup>a,\*</sup>, Syeda Alishwa Zaniab<sup>b</sup>, Sehrish Ramzan<sup>c</sup>, Aqsa Nazir<sup>d</sup>,  
Wasfi Shatanawi<sup>a,e,f,\*</sup>

<sup>a</sup> Department of Mathematics and Sciences, College of Humanities and Sciences, Prince Sultan University, Riyadh, 11586, Saudi Arabia

<sup>b</sup> Department of Mathematics, Riphah International University, Main Satyana Road, Faisalabad 44000, Pakistan

<sup>c</sup> Department of Mathematics, Government College University Faisalabad, Faisalabad 44000, Pakistan

<sup>d</sup> Department of Engineering and Computer Science, National University of Modern Languages, Islamabad 44000, Pakistan

<sup>e</sup> Department of Medical Research, China Medical University Hospital, China Medical University, Taichung, 40402, Taiwan

<sup>f</sup> Department of Mathematics, Faculty of Science, The Hashemite University, P.O Box 330127, Zarqa 13133, Jordan

## ARTICLE INFO

## Keywords:

Epidemic disease

Disease-free equilibrium point

Next-generation matrix

Local stability

Global stability

## ABSTRACT

Ebola Virus Disease (EVD) is a viral hemorrhagic fever that affects humans and other primates. It is characterized by rapid virus spread in a short period of time. The disease has the potential to spread to many different regions of the world. In this paper, we have developed a modified mathematical model of the Ebola virus, adding the quarantine population as a control strategy. The quarantine population  $F$  and parameters  $\rho_3$  represent the rate at which individuals enter the quarantine compartment, which is vital in controlling the virus spread within society. The conformable derivatives have been applied to the modified model to observe the behavior of individuals for fractional derivative values between 0.7 and 1. For a modified model, the threshold parameter ( $R_0$ ) has been determined using the Next-Generation Matrix (NGM) method. We have checked local and global stability at a disease-free equilibrium point using Routh-Herwitz (RH) criteria and Castillo-Chavez, respectively. Numerical results obtained through the Fourth-Order Runge Kutta Method (RK4) demonstrate, a decrease in the virus transmission rate after following the implementation of the quarantine strategy.

## 1. Introduction

Ebola Virus Disease (EVD), commonly known as Ebola Hemorrhagic Fever (EHF) [1,2], is a viral hemorrhagic fever that affects humans and other primates. Researchers have created mathematical models to understand better the dynamics of the Ebola virus and the necessary intervention strategies that must be implemented to battle the disease effectively due to the current epidemic. Mathematical analysis and modeling are essential to infectious disease epidemiology. Many mathematicians developed new idea for creating mathematical models to solve complex biological problems [3–8]. A stochastic Susceptible-Exposed-Infected-Recovered (SEIR) model was suggested by Chowell et al. (2004) [9]. This model matched the Ebola epidemic data from the Congo in 1995 and Uganda in 2000. In the presence of intervention, the basic reproduction rate for Congo was projected to be  $R_0 = 1.83$ , whereas it was  $R_0 = 1.34$  for Uganda. The same data for the pandemic outbreak in the Congo were utilized in a similar model developed by Ndonguza

\* Corresponding authors.

E-mail addresses: [nabbas@psu.edu.sa](mailto:nabbas@psu.edu.sa) (N. Abbas), [wshatanawi@psu.edu.sa](mailto:wshatanawi@psu.edu.sa) (W. Shatanawi).

<https://doi.org/10.1016/j.heliyon.2024.e35818>

Received 18 July 2023; Received in revised form 25 July 2024; Accepted 5 August 2024

Available online 9 August 2024

2405-8440/© 2024 The Authors. Published by Elsevier Ltd. This is an open access article under the CC BY-NC license (<http://creativecommons.org/licenses/by-nc/4.0/>).

et al. (2004) in [10], which produced a lower estimate for the basic reproduction number  $R_0 = 1.4$ . The stochastic model SEIR model proposed in [9] underwent an extension. Gomes et al. (2014) [11] developed a meta-population stochastic epidemic model for the 2014 Ebola Virus Disease outbreak. This model evaluated the danger of the outbreak's global spread. Their concept was created as an epidemic and mobility model for the entire world. The everyday airline passenger flow between more than 200 nations is integrated into the mobility model. It was applied to provide a stochastic, individual-based simulation of the global spread of the disease. In their study, community, hospital, and funeral services were utilized to depict transmission dynamics using the compartmental disease model. According to the findings, the basic reproduction number for the sick population's rapid, short-term growth rate in impacted West African nations is estimated to be 1.5–2.0. They also discovered that, despite monitoring and containment efforts, hospital visits and burial rituals account for most of the disease's total transmission. According to Meltzer et al. (2014) [12], the effectiveness of hospital-based therapies depends on the treatment facility's capacity and admission rate. Following the pandemic from 2013 to 2016, numerous Ebola Virus Disease scenarios were examined in mathematical models. The Ebola virus disease (EVD) outbreak in West Africa was one of the most severe public health crises in recent history. Ajelli et al. [13] conducted a computational modeling analysis of the Ebola epidemic in Guinea, providing valuable insights into the potential impact of vaccination programs on controlling the spread of the disease. Estimating the reproduction number ( $R_0$ ) during the outbreak is another critical aspect of understanding epidemic dynamics. Chowell and Nishiura [14] provided a comprehensive overview of the Ebola virus's transmission dynamics and control measures. Their work emphasizes the importance of timely intervention and robust public health strategies in managing such outbreaks. In addition to these perspectives, Nazir et al. [15] proposed an advanced conformable mathematical model for EVD, enhancing the understanding of the disease's behavior and spread in Africa. Their model introduced new dimensions to the mathematical modeling of Ebola, contributing to the broader efforts to control and eventually eliminate the disease. Ahmad and Abbas (2021) [16] developed a nonlinear model, termed Susceptible–Exposed–Infected–Quarantined–Recovered (SEIQR), to investigate the transmission dynamics of Ebola virus disease. In their model, an additional class of quarantined individuals was incorporated to assess the impact of quarantine strategies on the exposed population. Tadmon and Kengne (2022) [17] developed a comprehensive mathematical model for Ebola virus transmission. It incorporates control measures like a ban on bush meat, social distancing, hygiene, vaccine dynamics, and strategies such as quarantine and screening to combat the disease's spread effectively. Ismail, S. (2023) [18] proposed a mathematical model for exploring the dynamics of Ebola Virus Disease infection, accompanied by sensitivity analysis. The model comprises five non-linear ordinary differential equations, and the basic reproduction number ( $R_0$ ) calculation is derived using the next-generation matrix method. Abah et al. (2024) [19] conducted a mathematical analysis and simulation of Ebola virus disease spread, incorporating mitigation measures. Their model integrates quarantine and public education campaigns as effective control measures to combat the spread of the disease. Our research builds upon the model proposed by Nazir et al. (2020) [15] by addressing several gaps identified in the existing literature. While Nazir et al. focused on a SIR-type model to understand the transmission dynamics of Ebola Virus Disease and its pathogens, our enhancements introduce a quarantine population, denoted as  $F$ , along with additional parameters  $\rho_3$ ,  $w_1$ , and  $w_2$ . These modifications are strategically employed as control measures to provide a more comprehensive understanding of infection dynamics. By incorporating the quarantine compartment, our model aims to offer clearer insights into how quarantine affects infection rates, thus improving the effectiveness of intervention strategies and contributing to a more robust and actionable framework for managing the spread of Ebola Virus Disease. The model also considers Ebola virus pathogens (bacteria, viruses, or other microorganisms that cause disease) in the environment. This inclusion is significant as it can affect the spread of the disease, and any changes in the statistics will influence the final results. The hidden phenomenon of an infected individual recovering after a quarantine period has been uncovered. For greater accuracy, we apply conformable derivatives to the proposed model and observe behavior for values of derivatives between 0.7 and 1. Well-posedness has been confirmed in the developed model. The reproduction number  $R_0$  has been determined to understand the situation of Ebola Virus Disease. Local and global stability are also calculated at the disease-free equilibrium when  $R_0 < 1$ . The graphical behavior of given individuals using the RK-4 method has also been discussed. **Section 2:** This section will cover the quarantine-based Ebola Virus Disease transmission model. The reproduction number will be determined using the next-generation method. Local and global stability at the disease-free equilibrium are also discussed in this section. **Section 3:** In this section, the Ebola Virus Disease model's results and discussions will be discussed. **Section 4:** This section will cover the conclusion.

## 2. Model formulation

To look at how the Ebola Virus Disease spread, persisted, and recurred in Africa. There could be assumptions;

- i) Deceased human beings are one of the sources of Ebola Virus Disease virus distribution. Because they departed, dead people might spread the disease during burial ceremonies.
- ii) The disease can enter the environment through the urine and faeces of infected or deceased individuals.
- iii) Infection can be transmitted via direct touch and indirect interactions, such as contaminated environments and surfaces.
- iv) The presence of Ebola Virus Disease in the environment due to consuming infected bush meat.
- v) Permanent disease-induced immunity exists.

A mathematical model depicted in Fig. 1 has been developed based on the aforementioned assumptions. Parameter descriptions are provided in Table 1, and the system equations are as follows:

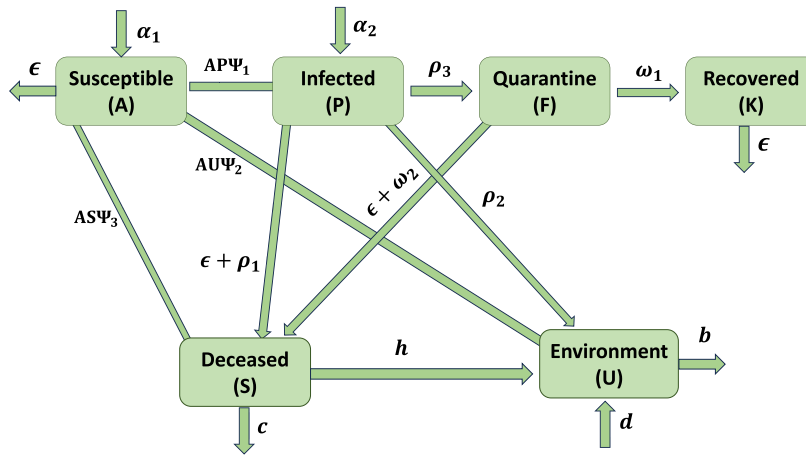


Fig. 1. Flowchart of EVD Model.

Table 1  
Physical Significant of Parameters.

Parameter	Description
$A$	Susceptible People
$P$	Infectious People
$F$	Quarantine People
$K$	Recovered Disease
$U$	Ebola virus Pathogens (a bacterium, virus or other microorganism, that causes disease) in the Environment
$S$	Deceased People
$\alpha_1$	The proportion at which Susceptible people are recruitment
$\alpha_2$	The proportion at which infected people are recruitment
$\psi_1$	The rate of contact (effective) of infected human
$\psi_2$	The rate contact of Ebola virus pathogens in the environment
$\psi_3$	Rate of contact (effective) of deceased (human)
$\epsilon$	Natural death rate of humans
$\rho_1$	Rate of deaths of human individuals due to infection
$\rho_2$	Rate at which shedding of infected humans
$\rho_3$	The rate at which infected people quarantined
$w_1$	The rate at which quarantined people are recovered
$w_2$	The rate at which quarantine people are in deceased
$h$	proportion of shedding of deceased people
$c$	The proportion rate of burial deceased people
$b$	The rate at which EVD in the environment

$$\begin{aligned}
 \frac{dA}{d\zeta} &= \alpha_1 - (\psi_1 P + \psi_3 S + \psi_2 U) A - \epsilon A, \\
 \frac{dP}{d\zeta} &= \alpha_2 + (\psi_1 P + \psi_3 S + \psi_2 U) A - (\rho_1 + \rho_2 + \rho_3 + \epsilon) P, \\
 \frac{dF}{d\zeta} &= \rho_3 P - (w_1 + w_2 + \epsilon) F, \\
 \frac{dK}{d\zeta} &= -\epsilon K + w_1 F, \\
 \frac{dU}{d\zeta} &= -bU + \rho_2 P + hS + d, \\
 \frac{dS}{d\zeta} &= (\epsilon + \rho_1) P + (w_2 + \epsilon) F - (h + c) S,
 \end{aligned}
 \tag{1}$$

with initial conditions,

$$A(0) \geq 0, P(0) \geq 0, F(0) \geq 0, K(0) \geq 0, U(0) \geq 0, S(0) \geq 0.$$

Let  $w : (0, \infty) \rightarrow \mathfrak{R}$  the conformable fractional derivative of  $g$  (of order  $\zeta$ ) can be defined as,

$$G_\zeta(g)(\zeta) = \lim_{\tau \rightarrow 0} \frac{w(\zeta + \tau t^{1-\zeta})}{\tau}. \tag{2}$$

The new definition, Eq. (2), also satisfies a few properties (mentioned in [20]). One of those properties is as follows, if  $w$  is differentiable, then,

$$G_{\zeta}(w)(\zeta) = t^{1-\zeta} \frac{dw}{d\zeta}.$$

The non-linear model (1), as Khalilzadeh’s conformable derivative [20], is as follows,

$$\begin{aligned} \frac{dA}{d\zeta} &= t^{\zeta-1}(\alpha_1 - (\psi_1 P + \psi_3 S + \psi_2 U) A - \epsilon A), \\ \frac{dP}{d\zeta} &= t^{\zeta-1}(\alpha_2 + (\psi_1 P + \psi_3 S + \psi_2 U) A - (\rho_1 + \rho_2 + \rho_3 + \epsilon) P), \\ \frac{dF}{d\zeta} &= t^{\zeta-1}(\rho_3 P - (w_1 + w_2 + \epsilon) F), \\ \frac{dK}{d\zeta} &= t^{\zeta-1}(-\epsilon K + (w_1 + \epsilon) F), \\ \frac{dU}{d\zeta} &= t^{\zeta-1}(-bU + \rho_2 P + hS + d), \\ \frac{dS}{d\zeta} &= t^{\zeta-1}((\epsilon + \rho_1) P + (w_2 + \epsilon) F - (h + c) S). \end{aligned} \tag{3}$$

Initial condition of non-linear system of equations,

$$A(0) = A_0, P(0) = P_0, K(0) = K_0, S(0) = S_0, U(0) = U_0, F(0) = F_0. \tag{4}$$

The conservation law is obtained by adding the first four equations of the above non-linear system of equations (3),

$$\frac{dH(\zeta)}{d\zeta} = t^{1-\zeta} (\alpha_1 + \alpha_2 - \epsilon(H) - (\rho_2 + \rho_3)P - (w_2 + c)F).$$

Let

$$H = A + P + F + K,$$

be the sum of the total alive /active population.

**Well-Posedness and Equilibria**

**Theorem 2.1.** Now suppose the non-linear system of equations (3) has a global solution for the initial condition (4), then the solution of the model remains non-negative for all time.

$$0 \leq A(0), 0 \leq P(0), 0 \leq F(0), 0 \leq K(0), 0 \leq S(0), 0 \leq U(0).$$

**Proof.** To demonstrate the non-negativity of the solution, we followed these steps: Let the first equation of the model be

$$\frac{dA}{d\zeta} = t^{\zeta-1}(\alpha_1 - (\psi_1 P + \psi_3 S + \psi_2 U) A - \epsilon A),$$

now let,  $T(\zeta) = (\psi_1 P + \psi_3 S + \psi_2 U) A - \epsilon$ , then,

$$\frac{dA}{d\zeta} = t^{\zeta-1}(\alpha_1 - A(\zeta)T(\zeta)). \tag{5}$$

The solution to equation (5) is a first-order linear equation in  $A$ .

$$A(\zeta) = A(0)e^{\int_0^\zeta T(c)-c^{\zeta-1} dc} + e^{\int_0^\zeta T(c)-c^{\zeta-1} dc} + \left( \int_0^\zeta \alpha_1 u^{\zeta-1} e^{\int_0^\zeta u^{\zeta-1} Q(u)du} du \right) \geq 0.$$

Which implies  $A(\zeta) \geq 0$  for all  $\zeta \geq 0$ . Similarly, other remaining equations have been proved. Then, the entire system is non-negative. □

**Theorem 2.2.** Given a positive set of solutions,  $(A(\zeta), P(\zeta), F(\zeta), K(\zeta))$ , there exists a domain in which the solution set is contained and bounded.

**Proof.** The total population of individuals are given,

$$H(\zeta) = A(\zeta) + P(\zeta) + F(\zeta) + K(\zeta),$$

$$\frac{dH}{d\zeta} = \frac{dA}{d\zeta} + \frac{dP}{d\zeta} + \frac{dF}{d\zeta} + \frac{dK}{d\zeta},$$

by simplification, we have,

$$\frac{dH}{d\zeta} = \alpha_1 + \alpha_2 - \epsilon(H) - (\rho_1 P + \rho_2 P + \omega_2 F),$$

$$\epsilon H(\zeta^*) \leq (\alpha_1 + \alpha_2 - \epsilon H(0))e^{-\epsilon \zeta^*},$$

$$H(\zeta^*) \leq \frac{\alpha_1 + \alpha_2}{\epsilon} - \frac{(\alpha_1 + \alpha_2 - \epsilon H(0))}{\epsilon} e^{-\epsilon \zeta^*}, \tag{6}$$

by taking the limit inequality (6) as  $\zeta^* \rightarrow \infty$  then we have,

$$H(\zeta^*) \leq \frac{\alpha_1 + \alpha_2}{\epsilon}.$$

Thus, we have  $H(\zeta^*) \leq \frac{\alpha_1 + \alpha_2}{\epsilon}$ , which shows that  $H \in \left[0, \frac{\alpha_1 + \alpha_2}{\epsilon}\right]$ . In other words,

$$\limsup_{t \rightarrow \infty} H(\zeta) = \frac{\alpha_1 + \alpha_2}{\epsilon},$$

and if  $H(\zeta) \leq \frac{\alpha_1 + \alpha_2}{\epsilon}$ , then  $H(\zeta)$  is bounded.  $\square$

The system of equations (3) is a dynamic system on the following compact set,

$$\begin{aligned} \Delta &= A(\zeta), P(\zeta), U(\zeta), S(\zeta), K(\zeta), F(\zeta) \in \mathbb{R}_6^+; \\ H_n &\leq \frac{\alpha_1 + \alpha_2}{\epsilon}, \\ S_n &\leq \frac{(\alpha_1 + \alpha_2)(\epsilon + \rho_2)w_1}{c\epsilon}, \\ U_n &\leq \frac{c\epsilon b + c\rho_3(\alpha_1 + \alpha_2) + h(\epsilon + \rho_2)(\alpha_1 + \alpha_2)}{c\epsilon w_1 d}. \end{aligned}$$

**Disease-Free Equilibrium Point**

In a mathematical model of disease transmission, a disease-free equilibrium point exists when no individuals in the population are infected with the disease. It represents a moment in time or a scenario where the disease has been effectively controlled or has not yet initiated its spread within the population. The disease-free equilibrium point is commonly utilized as a baseline for studying disease dynamics in various epidemiological models [21]. The disease-free equilibrium point of model is (3),

$$\Gamma_0 = (A, P, F, K, U, S) = \left(\frac{\alpha_1}{\epsilon}, 0, 0, 0, 0, 0\right).$$

**2.1. Reproduction number**

The basic reproductive number  $R_0$  is a crucial epidemiological parameter used to measure the transmission potential of infectious diseases within a population. It indicates the average number of secondary infections generated by a single infected individual in a fully susceptible population. To compute the basic reproduction number, we employ the next-generation matrix approach outlined in [22], utilizing the disease equations derived from the system of equations (3). Our focus is specifically on the infectious stages represented by  $A$ . We construct the transmission vector  $T$  to represent new infections, and the transition vector  $V$  to denote the outflow from the infectious compartments in (3), given by:

$$T = \begin{bmatrix} (\psi_1 p + \psi_3 s + \psi_2 u) a \\ 0 \\ 0 \\ 0 \\ 0 \end{bmatrix}, V = \begin{bmatrix} (\rho_1 + \rho_2 + \rho_3 + \epsilon) p \\ -\rho_3 p + (w_1 + w_2 + \epsilon + c) f \\ \epsilon k - w_1 f \\ bu - hs - \rho_2 p - d \\ -(\epsilon + \rho_1) p - w_2 f + (h + c) s \end{bmatrix}.$$

By substituting the values of  $\Gamma_0 = (A, P, F, K, U, S) = \left(\frac{\alpha_1}{\epsilon}, 0, 0, 0, 0, 0\right)$ , we calculate the Jacobian  $T$  from  $R$ , as follows:

$$R = \begin{bmatrix} \frac{\psi_1 \alpha_1}{\epsilon} & 0 & 0 & \frac{\psi_2 \alpha_1}{\epsilon} & \frac{\psi_3 \alpha_1}{\epsilon} \\ 0 & 0 & 0 & 0 & 0 \\ 0 & 0 & 0 & 0 & 0 \\ 0 & 0 & 0 & 0 & 0 \\ 0 & 0 & 0 & 0 & 0 \end{bmatrix},$$

and the Jacobian  $V$  from  $Y$  given by,

$$Y = \begin{bmatrix} \rho_1 + \rho_2 + \rho_3 + \epsilon & 0 & 0 & 0 & 0 \\ -\rho_3 & w_1 + w_2 + \epsilon + c & 0 & 0 & 0 \\ 0 & -w_1 & \epsilon & 0 & 0 \\ -\epsilon - \rho_1 & -w_2 & 0 & h + c & 0 \\ -\rho_3 & 0 & 0 & -h & b \end{bmatrix}.$$

From this, the next-generation matrix can be calculated as  $R_0 = \rho(RY^{-1})$ . Finally, we obtain the basic reproduction number as follows:

$$R_0 = \frac{\alpha_1 \psi_2 ((M_2 u_1 - \rho_2) h + c \rho_2)}{M_1 \epsilon (h + c) b} + \frac{((h + c) \psi_1 + \psi_3 (\epsilon + \rho_1)) \alpha_1}{M_1 \epsilon (h + c)} + \frac{w_2 \rho_3 (b \psi_3 + h \psi_2) \alpha_1}{M_1 M_2 \epsilon (h + c) b},$$

where  $M_1 = \rho_1 + \rho_2 + \rho_3 + \epsilon$ , and  $M_2 = w_1 + w_2 + \epsilon + c$ . We observe that  $\psi_1, \psi_2$ , and  $\psi_3$  exhibit a direct proportionality with  $R_0$ . That is, an increase in  $\psi_1, \psi_2$ , or  $\psi_3$  leads to a corresponding increase in  $R_0$ . Conversely, the sum  $w_1 + w_2$  demonstrates an inverse proportionality to  $R_0$ . Hence, an increase in  $w_1 + w_2$  results in a decrease in  $R_0$ . This shows that when  $R_0 > 1$  the rate of the Ebola virus is unstable when  $R_0 < 1$  the Ebola virus is unstable.

### 2.2. Stability analysis at disease-free equilibrium

#### Local Stability

**Theorem 2.3.** *The system of equations (3), is locally asymptotically stable around  $\Gamma_0$  for  $R_0 < 1$ .*

**Proof.** Determining the local stability according to the sign of the real parts of the eigenvalues, we have used the Routh-Hurwitz Stability Criteria. Firstly, consider  $\Omega_1, \Omega_2, \Omega_3, \Omega_4$ , derived from equations (3).

$$\Omega_1 = \psi_1 P + \psi_3 S + \psi_2 U,$$

$$\Omega_2 = \rho_1 + \rho_2 + \rho_3 + \epsilon,$$

$$\Omega_3 = w_1 + w_2 + \epsilon,$$

$$\Omega_4 = h + c.$$

Taking Jacobian  $J_0$  of system of non-linear system of equations (3) at disease-free equilibrium point,

$$J_0 = \begin{bmatrix} -\epsilon - \Omega_1 & 0 & 0 & 0 & 0 & 0 \\ \Omega_1 & -\Omega_2 & 0 & 0 & 0 & 0 \\ 0 & \rho_3 & -\Omega_3 & 0 & 0 & 0 \\ 0 & 0 & w_1 & -\epsilon & 0 & 0 \\ 0 & \rho_2 & 0 & 0 & h & -b \\ 0 & \epsilon + \rho_1 & w_2 & 0 & -\Omega_4 & 0 \end{bmatrix}. \tag{7}$$

From the last expression, which is  $\Delta^2 + C_1 \Delta + C_2 = 0$  where  $C_1 = -h$  and  $C_2 = \Omega_4 b$ , we apply the Routh-Hurwitz criteria [23]. The eigenvalue of the Jacobian matrix (7) consists of the negative fundamental part if and only if  $C_k > 0$ , for  $k = (1, 2)$ . Hence, the system of equations (3) is locally asymptotically stable at disease-free equilibrium points,

$$= (-\Omega_1 - \epsilon - \Delta) (-\Omega_2 - \Delta) (-\Omega_3 - \Delta) (-\epsilon - \Delta) (\Delta^2 - \Delta h - \Omega_4 b). \tag{8}$$

By solving Eq. (8), for the value of  $\Delta$ , the first four roots are,  $\Delta_1 = -(\Omega_1 + \epsilon)$ ,  $\Delta_2 = -\Omega_2$ ,  $\Delta_3 = -\Omega_3$ ,  $\Delta_4 = -\epsilon$ , all the values are negative.

From the last expression, which is  $\Delta^2 + C_1 \Delta + C_2 = 0$  where  $C_1 = -h$  and  $C_2 = \Omega_4 b$ , we apply the Routh-Hurwitz criteria [23]. The eigenvalue of the Jacobian matrix (7) consists of the negative fundamental part if and only if  $C_k > 0$ , for  $k = (1, 2)$ . Hence, the system of equations (3) is locally asymptotically stable at disease-free equilibrium points.  $\square$

#### Global Stability

By using the theorem by Castillo-Chavez et al. [24], we can express it as follows.

$$\frac{dM_H}{dt} = F(M_H, N_H),$$

$$\frac{dN_H}{dt} = H(M_H, N_H),$$

where,

$$H(M_H, N_H) = 0,$$

when  $M_H \in R$  and  $N_H \in R^5$  represent the system's DFEP, the uninfected and infected population, respectively.  $\Gamma_0 = (X^0, 0) = (A, 0, 0, 0, 0, 0)$ , where  $X^0 = \frac{\alpha_1}{\epsilon}$ . The epidemiological model's prerequisite for global stability at the disease-free equilibrium point (DFEP) is provided by,

$$\frac{dM_H}{dt} = F(M_H, 0) = 0, \tag{9}$$

$$H(M_H, N_H) = P_H N_{N^*} - \hat{H}(M_H, N_H). \tag{10}$$

**Theorem 2.4.** *The DEF point  $\Gamma_0$  of the system of equations (3) are globally asymptotically stable if  $R_0$  is less than unity.*

**Proof.** To prove condition (9), the model (3) can be set by, the disease-free equilibrium point is given,

$$\Gamma_0 = (X^0, 0) = \left(\frac{\alpha_1}{\epsilon}, 0, 0, 0, 0, 0\right),$$

and the system,

$$\frac{dM_H}{dt} = F(M_H, 0),$$

$$\frac{dA^*}{dt} = \alpha_1 - (\epsilon)A. \tag{11}$$

By solving equation (11), we find that the equation has a unique equilibrium point.

$$\left(A^* = \frac{\alpha_1}{\epsilon}\right),$$

hence,  $X^0$  is globally asymptotically stable for the condition (9) is satisfied.

Now, to verify the second condition (10).

$$H(M_H, N_H) = P_H N_{N^*} - \hat{H}(M_H, N_H),$$

and

$$\hat{H}(M_H, N_H) \geq 0,$$

$$H(M_H, N_H) = \begin{bmatrix} \alpha_2 + (\psi_1 P + \psi_3 S + \psi_2 U) A - (\rho_1 + \rho_2 + \rho_3 + \epsilon) P \\ \rho_3 P - (w_1 + w_2 + \epsilon) F \\ -\epsilon K + F w_1 \\ -bU + \rho_3 P + hS + d \\ (\epsilon + \rho_1) P + (w_2 + \epsilon) F - (h + \epsilon) S \end{bmatrix},$$

$$N_N^* = \begin{bmatrix} A^* \psi_1 - \epsilon - \rho_1 - \rho_2 - \rho_3 & 0 & 0 & \psi_2 A^* & \psi_3 A^* \\ \rho_3 & -w_1 - w_2 - \epsilon & 0 & 0 & 0 \\ 0 & w_1 & -\epsilon & 0 & 0 \\ \rho_2 & 0 & 0 & -b & h \\ \epsilon + \rho_1 & w_2 + \epsilon & 0 & 0 & -h - c \end{bmatrix},$$

$$\hat{H}(M_H, N_H) = \begin{bmatrix} (\psi_1 P + \psi_3 S + \psi_2 U) (A^* - A) \\ 0 \\ 0 \\ (\rho_2 - \rho_3) P - d \\ 0 \end{bmatrix},$$

this shows that,

$$\hat{H}(M_H, N_H) \geq 0.$$

As a result, if criteria (9)-(10) are met, the disease-free equilibrium point (DFEP)  $\Gamma_0$  is globally asymptotically stable when  $R_0 < 1$ . This is shown by Theorem 2.4.

Then, this proof is completed.  $\square$

### 3. Numerical result

The system of non-linear differential equation (3), has been solved using RK4 method [25]. We employ the Fourth-Order Runge Kutta Method (RK4) for fractional-order problems by employing Grunwald-Letnikov [26] for fractional derivatives. The fundamental concept is that using fractional order (represented by the parameter ‘ $\zeta$ ’) in these equations exposes memory effects not seen in mathematical models with ‘ $\zeta = 1$ ’ (corresponding to integer order models). In other words, fractional order models [15] contain hidden phenomena associated with memory effects that are not visible when ordinary differential equations with integer orders are used. To validate the theoretical findings presented in this study, numerical simulations were conducted using Maple 2019 computational software. The initial conditions for the variables  $A, P, F, K, U,$  and  $S$  were set as follows:  $A(0) = 0.9, P(0) = 0.8, K(0) = 0.2, S(0) = 0.5, F(0) = 0.1, U(0) = 0$ . These values represent the starting states of each variable at the onset of the model simulation. Table 2 provides a comprehensive overview of the parameter values used in the model, essential for accurately simulating and analyzing the dynamic interactions within the system. These initial conditions reflect the starting values of the variables in our system. Additionally, the simulations were carried out over 300 days, allowing us to observe the dynamic behavior of the system over an appropriate duration shown in Figs. 2-7.

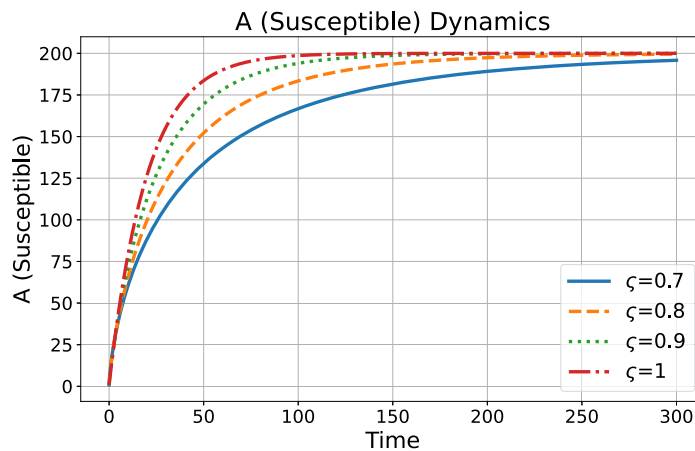


Fig. 2. Susceptible Dynamics  $A(\zeta)$ .

Fig. 2 shows the behavior of susceptible class for of  $\zeta = 0.7, 0.8, 0.9, 1$ . This Plot shows that, when we apply quarantine strictly, the rate of susceptible individuals are going to increase.

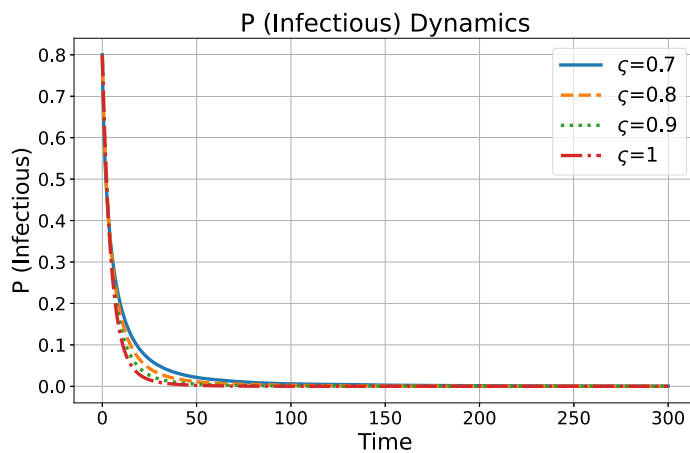


Fig. 3. Infectious Dynamics  $P(\zeta)$ .

Fig. 3 shows the behavior of infectious individuals for different values of  $\zeta$ . This plot shows that the rate of infectious is going to decrease when we apply quarantine strictly.



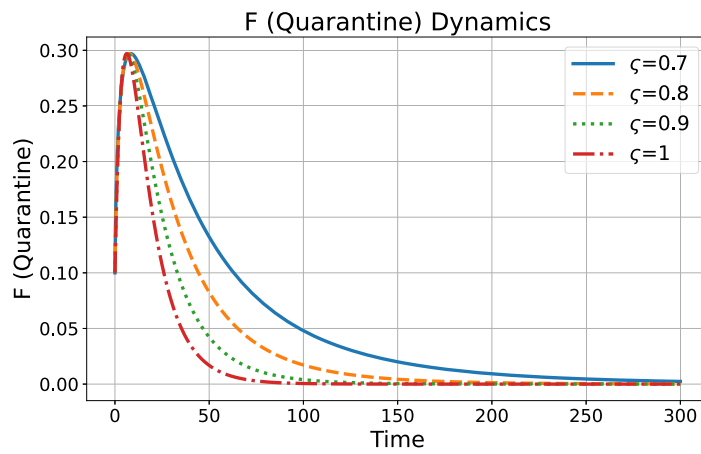


Fig. 4. Quarantine Dynamics  $F(\zeta)$ .

Fig. 4 shows the behavior of quarantine class for different values of  $\zeta$ . This plot shows that as the rate of infection decreases, the rate of quarantine people also decreases after the passage of time.

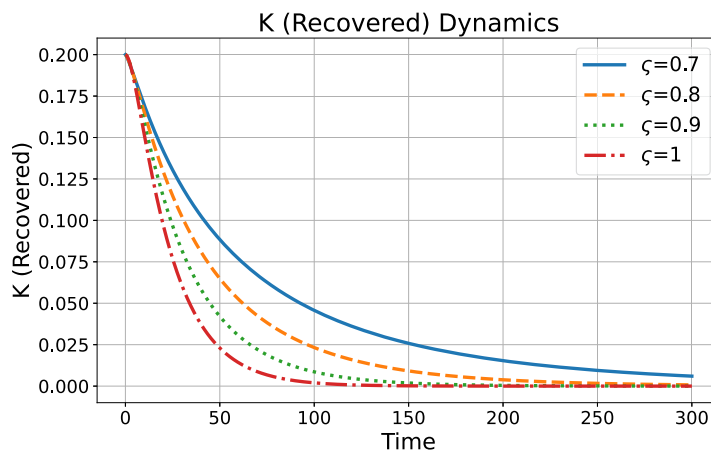


Fig. 5. Recovered Dynamics  $K(\zeta)$ .

Fig. 5 shows the behavior of recovered class for different values of  $\zeta$ . This plot shows that as the rate of quarantine people decreases, the rate of recovered people also decreases.

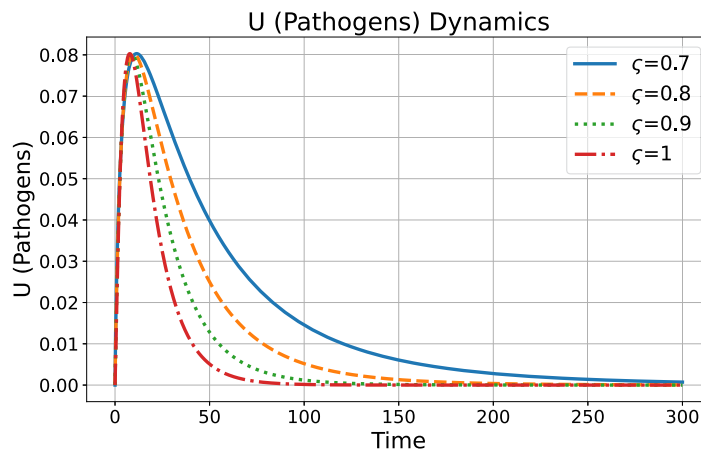


Fig. 6. Ebola Virus Pathogens in the Environment  $U(\zeta)$ .

Fig. 6 shows the behavior of Ebola virus pathogens in the environment for different values of  $\zeta$ . This plot shows that the rate of Ebola virus pathogens and the infection rate will also decrease.

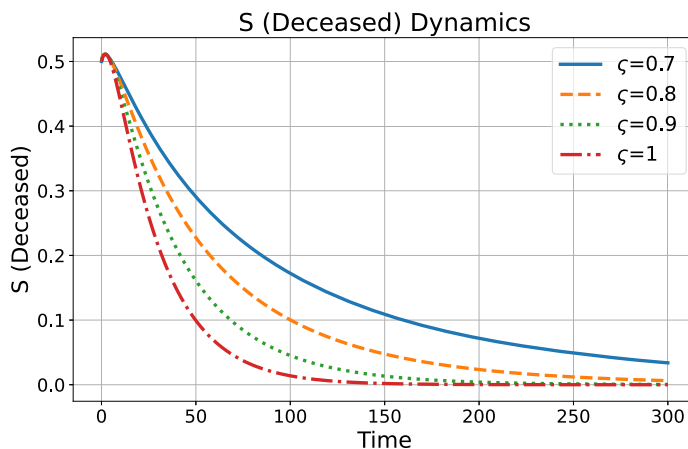


Fig. 7. Deceased Dynamics  $S(\zeta)$ .

Fig. 7 shows the behavior of deceased class for different values of  $\zeta$ . This plot shows that as Ebola virus pathogen decrease and infectious decrease, there's a corresponding decrease in deceased dynamics.

Table 2  
Estimated Values of Parameters.

Parameters	Values	Sources
$\alpha_1$	10	[15]
$d$	0.0015	[15]
$\alpha_2$	3	[15]
$\psi_1$	0.006	[15]
$\psi_2$	0.0012	[15]
$b$	0	[15]
$\psi_3$	0.006	[15]
$c$	0.8	[15]
$e$	0.5	[15]
$h$	0.04	[15]
$\rho_1$	0.123	Assumed
$w_1$	0.04	Assumed
$\rho_2$	0.04	[15]
$w_2$	0.22	Assumed
$\rho_3$	0.12	Assumed

### 3.1. Discussion

Nazir et al. (2020) [15] utilized conformable derivatives to develop a susceptible-infected-recovered (SIR)-type model for exploring the transmission dynamics of Ebola Virus Disease (EVD) and Ebola virus pathogens in the environment. Our investigation highlighted the pivotal role of introducing a quarantine population ( $F$ ) in controlling the Ebola virus. Recognizing its significance, we extended their work by incorporating a modified model with additional parameters ( $\rho_3$ ,  $w_1$ , and  $w_2$ ) that govern the rates at which individuals enter the quarantined compartment. Using conformable derivatives made the model more realistic, especially by showing that infected individuals could recover after quarantine, as shown in Figs. 2 to 7. We observed that as the number of infections, shown in Fig. 3, increased, so did the rate of quarantine, illustrated in Fig. 4, leading to a corresponding rise in recovered individuals shown in Fig. 5. Increasing rates like  $\rho_3$  and  $w_2$  accelerated the quarantining process, thereby augmenting the recovery rate. Numerical simulations conducted using Maple 2019 underscored our model's applicability. By integrating quarantine measures, our study offers a more practical approach to managing Ebola Virus Disease outbreaks. Importantly, our model aligns existing literature [15,16] when the modification factor is excluded, ensuring credibility and making it easier to compare Ebola Virus Disease transmission dynamics.

### 4. Conclusion

In this paper, we examined how Ebola Virus Disease spreads using a modified mathematical model with a quarantined class  $F(\zeta)$ . As, the quarantined class plays an important role in the control of the Ebola virus because it isolates affected persons and prevents

disease spread. A system of nonlinear conformable differential equations has been used to determine the problem, and a well-known theorem has been applied to ensure its well-posedness. We also have calculated the basic reproduction number using the next-generation matrix method. Local and global stability analysis have observed at a disease-free equilibrium point using Routh-Hurwitz (RH) criteria and Castillo-Chavez, respectively. Numerical results obtained via the Fourth-Order Runge Kutta Method (RK4) provided information into the behavior of individuals for fractional derivative values between 0.7 to 1. As the number of infected people increases, the rate of quarantine also increases, leading to an increase in the number of recovered individuals. Numerical simulations indicate a decrease in the virus transmission rate after implementing quarantine measures. Additionally, we have concluded that, to control the spread of Ebola Virus Disease, infected persons should be kept quarantined, and dead bodies should be buried carefully. The absence of Ebola Virus Disease transmission from the environment can significantly contribute to a population free of disease. Future research should explore the impact of varying quarantine durations and adherence levels on disease control effectiveness using optimal control strategies. Alternatively, applying other fractional derivatives could enhance the results. These areas represent potential shortcomings of the present work that require further investigation.

## Funding

No funding.

## CRediT authorship contribution statement

**Nadeem Abbas:** Writing – review & editing, Writing – original draft, Data curation, Conceptualization. **Syeda Alishwa Zanib:** Writing – review & editing, Writing – original draft, Validation, Methodology, Formal analysis. **Sehrish Ramzan:** Writing – review & editing, Writing – original draft, Validation, Investigation, Data curation. **Aqsa Nazir:** Validation, Supervision, Software, Resources. **Wasfi Shatanawi:** Supervision, Software, Resources, Investigation.

## Declaration of competing interest

All the authors have no declaration of interest in the manuscript.

## Data availability

No data was used for the research described in the article.

## Acknowledgements

The authors would like to thank Prince Sultan University for their support through the TAS research lab.

## References

- [1] S.T. Jacob, I. Crozier, W.A. Fischer, A. Hewlett, C.S. Kraft, M.A.D.L. Vega, M.J. Soka, V. Wahl, A. Griffiths, L. Bollinger, J.H. Kuhn, Ebola virus disease, *Nat. Rev. Dis. Primers* 6 (1) (2020) 13, <https://doi.org/10.1038/s41572-020-0147-3>.
- [2] M.D. Ahmad, M. Usman, A. Khan, M. Imran, Optimal control analysis of Ebola disease with control strategies of quarantine and vaccination, *Infect. Dis. Poverty* 5 (2016) 1–12, <https://doi.org/10.1186/s40249-016-0161-6>.
- [3] S.A. Zanib, S. Ramzan, N. Abbas, et al., A mathematical approach to drug addiction and rehabilitation control dynamic, *Model. Earth Syst. Environ.* (2024) 1–8, <https://doi.org/10.1007/s40808-023-01931-y>.
- [4] J.P. Singh, T. Abdeljawad, D. Baleanu, S. Kumar, Transmission dynamics of a novel fractional model for the Marburg virus and recommended actions, *Eur. Phys. J. Spec. Top.* 232 (14) (2023) 2645–2655, <https://doi.org/10.1140/epjs/s11734-023-00943-0>.
- [5] P.A. Naik, Global dynamics of a fractional-order SIR epidemic model with memory, *Int. J. Biomath.* 13 (08) (2020) 2050071, <https://doi.org/10.1142/s1793524520500710>.
- [6] M.B. Ghorri, P.A. Naik, J. Zu, Z. Eskandari, M.U.D. Naik, Global dynamics and bifurcation analysis of a fractional-order SEIR epidemic model with saturation incidence rate, *Math. Methods Appl. Sci.* 45 (7) (2022) 3665–3688, <https://doi.org/10.22541/au.162530373.38917682/v1>.
- [7] A. Ahmad, M. Farman, P.A. Naik, N. Zafar, A. Akgul, M.U. Saleem, Modeling and numerical investigation of fractional-order bovine babesiosis disease, *Numer. Methods Partial Differ. Equ.* 37 (3) (2021) 1946–1964, <https://doi.org/10.1002/num.22632>.
- [8] F. Evirgen, E. Uçar, N. Özdemir, E. Altun, T. Abdeljawad, The impact of nonsingular memory on the mathematical model of Hepatitis C virus, *Fractals* 31 (04) (2023) 2340065, <https://doi.org/10.1142/S0218348X23400650>.
- [9] G. Chowell, N.W. Hengartner, C. Castillo-Chavez, P.W. Fenimore, J.M. Hyman, The basic reproductive number of Ebola and the effects of public health measures: the cases of Congo and Uganda, *J. Theor. Biol.* 229 (1) (2004) 119–126, <https://doi.org/10.1016/j.jtbi.2004.03.006>.
- [10] D. Ndanguza, I.S. Mbalawata, H. Haario, J.M. Tchuente, Analysis of bias in an Ebola epidemic model by extended Kalman filter approach, *Math. Comput. Simul.* 142 (2) (2017) 113–129, <https://doi.org/10.1016/j.matcom.2017.05.005>.
- [11] C. Poletto, M.F. Gomes, A. Pastore y Piontti, L. Rossi, L. Bioglio, D.L. Chao, I.M. Longini, M.E. Halloran, V. Colizza, A. Vespignani, Assessing the impact of travel restrictions on the international spread of the 2014 West African Ebola epidemic, *Euro Surveill.* 19 (42) (2014) 20936, <https://doi.org/10.2807/1560-7917.es2014.19.42.20936>.
- [12] M.I. Meltzer, C.Y. Atkins, S. Santibanez, B. Knust, B.W. Petersen, E.D. Ervin, M.L. Washington, Estimating the future number of cases in the Ebola epidemic—Liberia and Sierra Leone, 2014–2015, *Morb. Mort. Wkly. Rep.* 63 (3) (2014) 1–20, PMID: 25254986.
- [13] M. Ajelli, S. Merler, L. Fumanelli, A. Pastore y Piontti, N.E. Dean, I.M. Longini, A. Vespignani, Spatiotemporal dynamics of the Ebola epidemic in Guinea and implications for vaccination and disease elimination: a computational modeling analysis, *BMC Med.* 14 (1) (2016) 1–10, <https://doi.org/10.1186/s12916-016-0678-3>.

- [14] G. Chowell, H. Nishiura, A review of transmission dynamics and control of Ebola virus disease (EVD), *BMC Med.* 12 (1) (2014) 1–17, <https://doi.org/10.1186/s12916-014-0196-0>.
- [15] A. Nazir, N. Ahmed, U. Khan, S.T. Mohyud-Din, K.S. Nisar, I. Khan, An advanced version of a conformable mathematical model of Ebola virus disease in Africa, *Alex. Eng. J.* 59 (5) (2020) 3261–3268, <https://doi.org/10.1016/j.aej.2020.08.050>.
- [16] W. Ahmad, M. Abbas, Effect of quarantine on transmission dynamics of Ebola virus epidemic: a mathematical analysis, *Eur. Phys. J. Plus* 136 (4) (2021) 1–33, <https://doi.org/10.1140/epjp/s13360-021-01360-9>.
- [17] C. Tadmon, J.N. Kengne, Mathematical analysis of a model of Ebola disease with control measures, *Int. J. Biomath.* 15 (07) (2022) 2250048, <https://doi.org/10.1142/S1793524522500486>.
- [18] S. Ismail, Mathematical analysis of in-host Ebola virus infection dynamics model with sensitivity analysis, *Ethiop. J. Sci. Technol.* 16 (3) (2023) 181–207, <https://doi.org/10.1016/j.fraope.2023.100066>.
- [19] R.T. Abah, A.B. Zhiri, K. Oshinubi, A. Adeniji, Mathematical analysis and simulation of Ebola virus disease spread incorporating mitigation measures, *Franklin Open* 6 (2024) 100066, <https://doi.org/10.1016/j.fraope.2023.100066>.
- [20] R. Khalil, M. Al Horani, A. Yousef, M. Sababheh, A new definition of fractional derivative, *J. Comput. Appl. Math.* 264 (2014) 65–70, <https://doi.org/10.1016/j.cam.2014.01.002>.
- [21] J.C. Kamgang, G. Sallet, Computation of threshold conditions for epidemiological models and global stability of the disease-free equilibrium (DFE), *Math. Biosci.* 213 (1) (2008) 1–12, <https://doi.org/10.1016/j.mbs.2008.02.005>.
- [22] O. Diekmann, J.A.P. Heesterbeek, M.G. Roberts, The construction of next-generation matrices for compartmental epidemic models, *J. R. Soc. Interface* 7 (47) (2010) 873–885, <https://doi.org/10.1098/rsif.2009.0386>.
- [23] E.X. DeJesus, C. Kaufman, Routh-Hurwitz criterion in examining eigenvalues of a system of nonlinear ordinary differential equations, *Phys. Rev. A* 35 (12) (1987) 5288, <https://doi.org/10.1103/PhysRevA.35.5288>.
- [24] C. Castillo-Chavez, S. Blower, P. Van den Driessche, D. Kirschner, A.A. Yakubu (Eds.), *Mathematical Approaches for Emerging and Reemerging Infectious Diseases: Models, Methods, and Theory* (vol. 126), Springer Science and Business Media, New York, USA, 2002, pp. 1–368.
- [25] J.C. Butcher, On the implementation of implicit Runge-Kutta methods, *BIT Numer. Math.* 16 (3) (1976) 237–240, <https://doi.org/10.1007/BF01932774>.
- [26] M.S. Abdelouahab, N.E. Hamri, The Grünwald–Letnikov fractional-order derivative with fixed memory length, *Mediterr. J. Math.* 13 (2) (2016) 557–572, <https://doi.org/10.48550/arXiv.1304.0616>.